Nonmagnetic–magnetic transition in $Yb(Cu_{1-x}Ni_x)_2Si_2$ studied by muon-spin relaxation

2003 J. Phys.: Condens. Matter 15 6997

(http://iopscience.iop.org/0953-8984/15/41/009)

INSTITUTE OF PHYSICS PUBLISHING JOURNAL OF PHYSICS: CONDENSED MATTER

J. Phys.: Condens. Matter **15** (2003) 6997–7017 PII: S0953-8984(03)66332-0

Nonmagnetic–magnetic transition in $Yb(Cu_{1-x}Ni_x)_2Si_2$ studied by muon-spin relaxation

D Andreica[1,3], A Amato[2], F N Gygax[1] and A Schenck[1]

[1] Institute for Particle Physics, ETH Zurich, CH-5232 Villigen PSI, Switzerland
[2] Laboratory for Muon Spin Spectroscopy, Paul Scherrer Institute, CH-5232 Villigen PSI, Switzerland

E-mail: dandr@phys.ubbcluj.ro

Received 15 July 2003, in final form 9 September 2003
Published 3 October 2003
Online at stacks.iop.org/JPhysCM/15/6997

Abstract

The muon-spin relaxation technique has been used to investigate the transition from a nonmagnetic to a magnetic ground state in $Yb(Cu_{1-x}Ni_x)_2Si_2$. The effect of the chemical substitution of Cu by Ni on the magnetic properties is evidenced by an unusual occurrence of magnetic ordering, characterized by an x-dependent magnetic volume fraction. Both the magnetic transition temperature and the magnetic volume fraction are observed to increase with Ni concentration. It is found that the size of the magnetic volume fraction depends on the probability of an Yb ion possessing at least two Ni ions as nearest neighbours. The transition temperature of $YbNi_2Si_2$ is shown to be reduced compared to that of the pressurized $YbCu_2Si_2$ at equivalent volume and is related to electron doping effects. Using a scaling law for the temperature dependence of the relaxation rates of the Yb-moments, the Kondo temperature is deduced and found to decrease, as expected, with increasing Ni concentration.

1. Introduction

In numerous Ce, Yb and U compounds, generally called Kondo lattices, competing interactions lead to a wealth of magnetic ground states. The low temperature ground state properties of these compounds are strongly influenced by the degree of hybridization between the localized f states and the conduction-band states. Competition occurs between the demagnetizing Kondo interaction and the Ruderman–Kittel–Kasuya–Yosida (RKKY) indirect interaction between localized moments. Whereas the former interaction leads to a dynamic screening of the localized magnetic moments, i.e., promotes a nonmagnetic ground state, the later favours the formation of a magnetic ground state. In a simple picture, the competition between

[3] Permanent address: Faculty of Physics, Babeş-Bolyai University, 3400 Cluj-Napoca, Romania.

these interactions can be treated in the frame of the 'Kondo-necklace' model developed by Doniach [1].

A current issue is the understanding of the ground state properties of Ce and Yb compounds close to the magnetic–nonmagnetic borderline. The hybridization between the f states and the conduction electron states, which controls the RKKY and Kondo interactions differently, can be tuned either by applying an external pressure or by changing the volume of the unit cell by chemical substitution.

The compound $YbCu_2Si_2$ is of particular interest since it shows the occurrence of pressure-induced magnetism for values of the applied pressure above a critical pressure of about 80 kbar [2]. At zero pressure $YbCu_2Si_2$ is an intermediate valence (IV) compound characterized by a nonmagnetic ground state and an enhanced specific heat coefficient. The Sommerfeld coefficient γ of the specific heat is equal to 135 mJ mol^{-1} K^{-2} [3] and the valence of the Yb ion is found to be close to 2.8 at 4 K [4]. On the other side of the $Yb(Cu_{1-x}Ni_x)_2Si_2$ series, $YbNi_2Si_2$ is an antiferromagnet below $T_N = 2.1$ K [5], characterized by a helical magnetic structure [6] and possessing a crystallographic unit cell volume smaller than that of $YbCu_2Si_2$.

In the present paper, we report μSR results concerning the effect of the chemical substitution (Ni/Cu) on the magnetic properties $YbCu_2Si_2$. We show that for $Yb(Cu_{1-x}Ni_x)_2Si_2$ a critical concentration—equivalent to critical pressure—between magnetic and nonmagnetic ground states cannot be defined.

2. Experimental details

Nine polycrystalline $Yb(Cu_{1-x}Ni_x)_2Si_2$ samples ($x = n \times 0.125$ with n ranging from 0 to 8) were prepared in collaboration with Dr Alami-Yadri from the Université de Genève, using a sealed tube method [7]. The starting elements were Yb 4N from Ames Laboratories, USA, and Cu 6N, Ni 6N and Si 6N from Fluka, Switzerland. Optical microscopy measurements and x-ray diffraction were employed to check for the homogeneity of the samples inside the tube and to determine the x-dependence of the lattice parameters. Several samples suitable for transport properties [8–10], magnetic susceptibility and μSR measurements [9, 11] were then cut from the selected disks.

The bulk of the μSR experiments were performed at the SμS (Swiss Muon Source, Paul Scherrer Institute, Switzerland), using the GPS, LTF, DOLLY and GPD spectrometers. A few measurements, with the $x = 0$ and 0.125 samples, were also performed using the EMU μSR beam line at ISIS (UK). μSR spectra were recorded using the zero-field (ZF) and longitudinal field (LF, up to 6 kG) configurations in a temperature range of 0.04–300 K.

3. Results and discussion

The ZF μSR spectra recorded in the paramagnetic phase of $Yb(Cu_{1-x}Ni_x)_2Si_2$ are best fitted using a product of a stretched exponential and a Kubo–Toyabe depolarization function:

$$P_z(t) = [\tfrac{1}{3} + \tfrac{2}{3}(1 - \Delta^2 t^2)e^{-\Delta^2 t^2/2}] \exp[-(\lambda_{ZF} t)^{\beta}]. \quad (1)$$

This equation describes a two-channel depolarization process acting on the muon spin. The first channel arises from the static—in the time window of the μSR experiment—nuclear magnetic moments ($Yb^{171,173}$, $Cu^{63,65}$, Ni^{61} and Si^{29}) and is evidenced by the term in square brackets of $P_z(t)$ which represents a Kubo–Toyabe contribution [12]. The second channel is ascribed to the fluctuations of the Yb magnetic moments and is represented by the stretched exponential term. The parameter Δ describes the width of the static field distribution at the

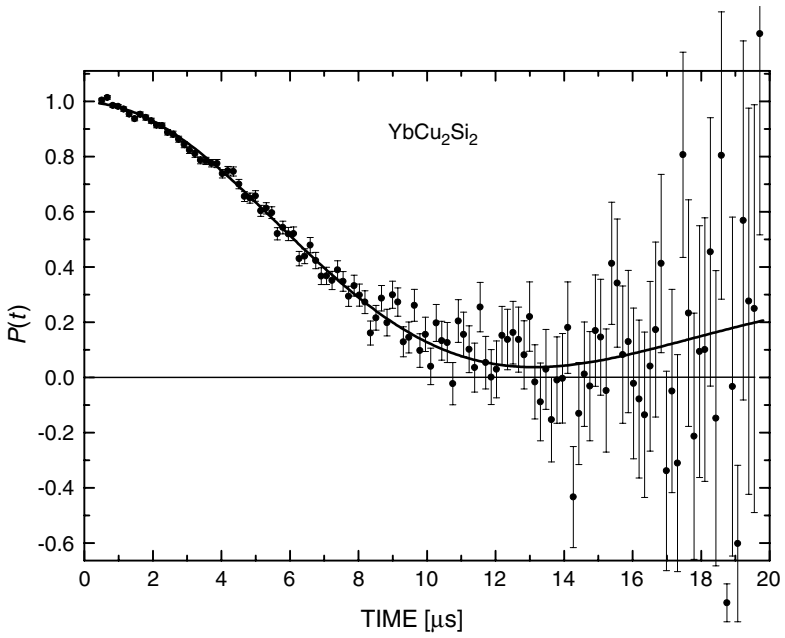

Figure 1. μSR signal measured for $YbCu_2Si_2$ at 5 K using the MORE facility at PSI. The signal was fitted using equation (1) with $\lambda_{ZF} = 0$ (the solid curve).

muon site created by the nuclear magnetic moments [13], λ_{ZF} is the ZF muon spin relaxation rate and β is a fit parameter associated with the spread/distribution of λ_{ZF} as discussed below.

The μSR spectra at low temperatures for $YbCu_2Si_2$ are well described by a Kubo–Toyabe depolarization function, as shown in figure 1. This indicates that the Yb electronic magnetic moments are fluctuating too fast to affect the muon polarization, corresponding to the limit $\lambda_{ZF} \approx 0$. As a consequence, solely the depolarization due to the static field distribution of the randomly oriented nuclear spins is observed. The μSR spectrum reported in figure 1 was recorded at 5 K using the MORE (muons on request, [14]) facility at PSI. On the other side of the series, the value of Δ is small for $YbNi_2Si_2$, producing μSR spectra that are quasi-exponential in shape as evidenced in figures 2 and 3.

3.1. The muon stopping site

The knowledge of the depolarization rate Δ provides information on the muon stopping site in the crystallographic unit cell. Due to Coulomb repulsion from the ions, the muon stops in symmetric interstitial sites. The depolarization rate Δ is related to the second moment of the field distribution [13] created, at the muon site, by the nuclear magnetic moments of Yb, Cu, Ni and Si. By comparing the measured and the calculated values of Δ it is therefore possible to determine the muon site.

The parameter Δ was calculated for several symmetry planes of the $ThCr_2Si_2$ structure. The natural abundance a_i (in %) of the isotopes was taken into account by weighing the corresponding second moment of the field distribution with a probability $p_i = a_i/100$. The measured values of Δ for different Ni concentrations are displayed in figure 4. They indicate a monotonous decrease with increasing Ni concentration x, in agreement with our calculations. The $\Delta(x)$-dependence of the relaxation rate, calculated for the 8g and the 4e sites, is also

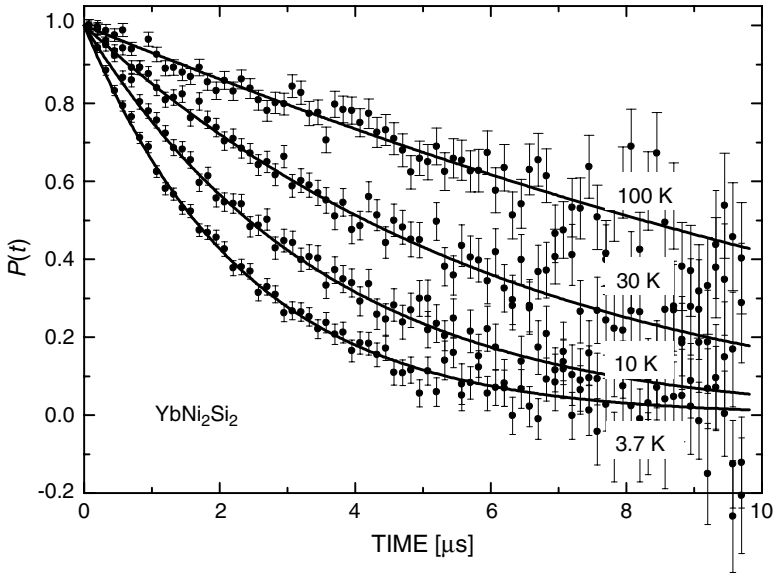

Figure 2. μ^+ depolarization in $YbNi_2Si_2$ at different temperatures above 3.2 K. The curves are fits of equation (1) to the μSR spectra ($\beta \cong 1$).

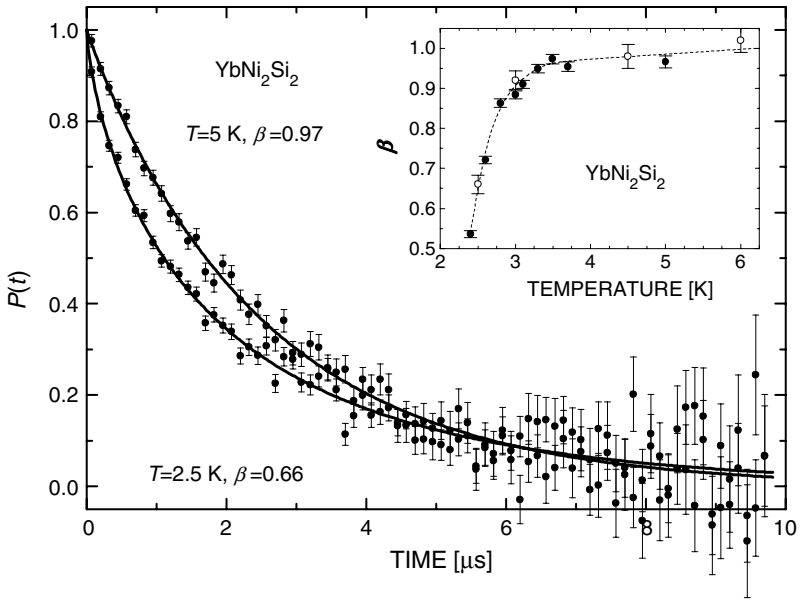

Figure 3. μSR signal for $YbNi_2Si_2$ at two temperatures. The curves are fits using equation (1). The inset shows the temperature dependence of β (see the text; different symbols represent results of measurements using different μSR spectrometers).

reported in figure 4. For both 8g and 4e sites, the value of $\Delta(x = 0)$ is close to the experimental value. For the 4e site a value of Δ of about 0.1 μs^{-1} is expected for $x = 1$, but it could not be observed (see figure 2). As shown in figure 4 the experimental data follow certainly not the x-dependence calculated for the 4e site. For low x-values the data possibly match the

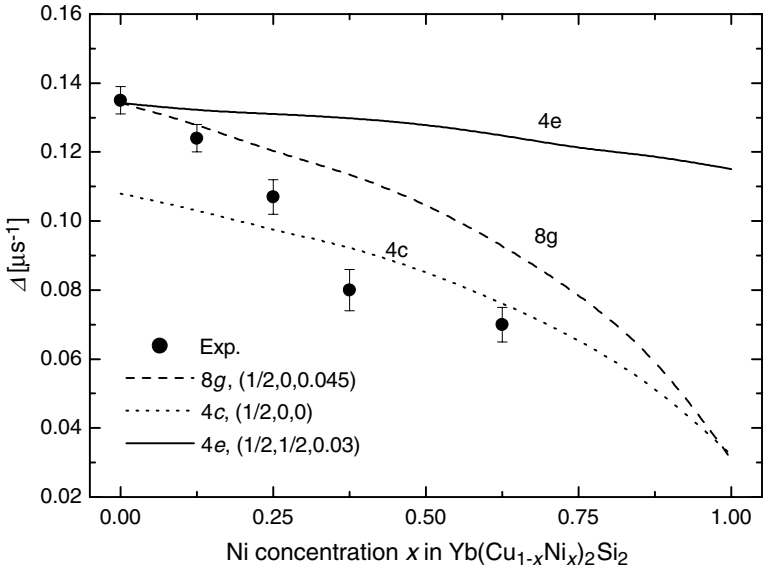

Figure 4. Calculated values of $\Delta(x)$ for $Yb(Cu_{1-x}Ni_x)_2Si_2$ considering different muon sites (curves). The experimental results are displayed with full circles.

8g curve, but they also deviate above $x = 0.25$. However, the possibility that the muon site (particularly the z-component) changes slightly as a function of the Ni concentration cannot be excluded. This is suggested in figure 4 by the dotted curve, which represents the calculated $\Delta(x)$-dependence for the $(1/2, 0, 0)$ site which roughly agrees with the data for $x > 0.25$. Another explanation for the observed behaviour would be that the muon occupies the 4e site for $x = 0$ and changes to the 4c site for $x > 0$.

The present site determination can be compared to the results obtained for Kondo lattice systems possessing the same tetragonal crystallographic structure. In $CeCu_2Si_2$, with almost the same lattice parameters as $YbCu_2Si_2$, a depolarization rate of $\Delta = 0.135\ \mu s^{-1}$ was observed, with similar temperature dependence [15]. The $(1/2, 1/2, 0)$ site was chosen as the muon site after considering the qualitative information obtained from muon Knight-shift data measured on a single crystal. The same $(1/2, 1/2, 0)$ muon site was found in $CeRu_2Si_2$ [16, 17]. In $CeRh_2Si_2$, $(1/2, 0, 0)$ was identified as the muon site based on the magnetic structure determined by neutron scattering and the ZF μSR measurements in the magnetically ordered phase. Therefore, for $Ce(Ru_{1-x}Rh_x)_2Si_2$ one could expect a site change from $(1/2, 1/2, 0)$ for $x = 0$ to $(1/2, 0, 0)$ for $x = 1$. In $Ce_{0.95}La_{0.05}Ru_2Si_2$ [18] the $(1/2, 0, 1/8)$ muon site was favoured among the 11 most probable sites of the tetragonal structure [19]. Finally, in $U(Pd_{1-x}Fe_x)_2Ge_2$ [20] the same $(1/2, 0, 1/8)$ site was again assigned to the muon.

With this information on the muon site we turn now to the discussion of the electronic magnetic moment contributions to the muon depolarization function—i.e., the second part of the right-hand side term of equation (1).

3.2. The stretched exponential fit

A stretched exponential depolarization function has been utilized in several cases. Muon-spin depolarization in spin glasses is successfully described by such a function [21]. However, the occurrence of a spin-glass state for the present compounds can be safely excluded

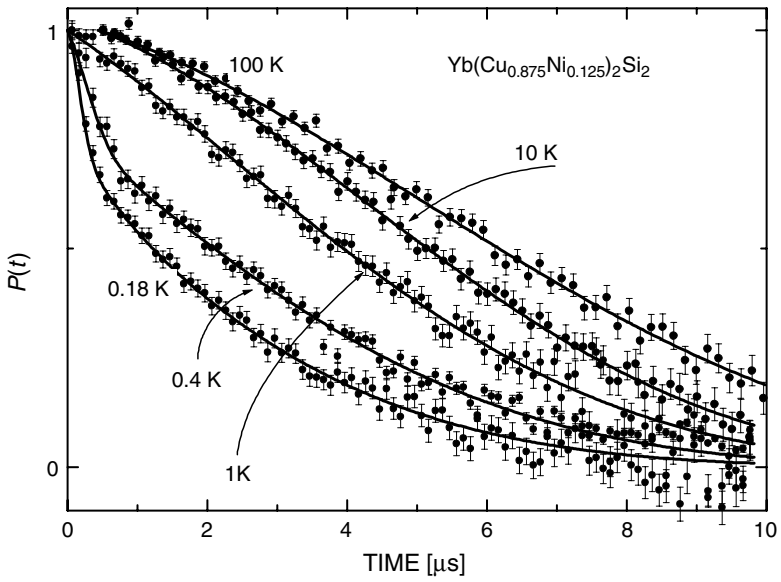

Figure 5. ZF μSR spectra for $Yb(Cu_{0.875}Ni_{0.125})_2Si_2$ at different temperatures below and above the magnetic transition ($T_m \gtrsim 0.5$ K). Notice the Gaussian shape of the depolarization at high temperatures. The curves are fits of the μSR spectra (see text).

since neutron scattering measurements [6] have shown that the ground state of $YbNi_2Si_2$ is clearly antiferromagnetic. Alternatively, a distribution of magnetic transition temperatures or anisotropy (and/or distribution) of the fluctuation rate of the magnetic moments can also be reflected by a stretched exponential depolarization function of the μSR signal (see [22] and references therein). The present μSR data do not permit us to distinguish between these two possibilities. Indeed, the fluctuations of the Yb magnetic moments might be anisotropic close to the magnetic phase transition, at least for $YbNi_2Si_2$ [23] (below T_N the moments are oriented in the *a–b* crystallographic plane [6]). On the other hand, the disorder induced by the chemical substitution can favour magnetic clustering close to the magnetic transition temperature, producing a distribution of fluctuation rates related to the cluster dimension and the value of the fluctuating moment. The disorder can also lead to a distribution of Kondo temperatures T_K reflected in turn by a distribution of transition temperatures T_m. The fluctuation rate distribution, in this case, is given by the distribution of $(T - T_m)$ at each value of T.

In $Yb(Cu_{1-x}Ni_x)_2Si_2$ (for $x > 0$) β differs from unity only in a small temperature region above the transition temperature (see the inset of figure 3). Typical μSR spectra as well as the temperature dependence of the parameter β for $x = 0.875$ are displayed in figures 5 and 6, respectively. For all the concentrations, the parameter β is found to be constant and equal to unity down to about 10 K. Upon further lowering of the temperature, a slight decrease of β is observed.

The temperature dependence of the depolarization rate λ_{ZF} for different Ni concentrations is presented in figure 7 in a double logarithmic plot. For all the samples, a similar power-like $\lambda_{ZF}(T)$-dependence is observed at high temperatures. Below 2 K, the fast increase of the relaxation rate is due to the slowing down of the Yb^{3+} spin fluctuations upon decreasing the temperature toward the magnetic transition temperature T_m.

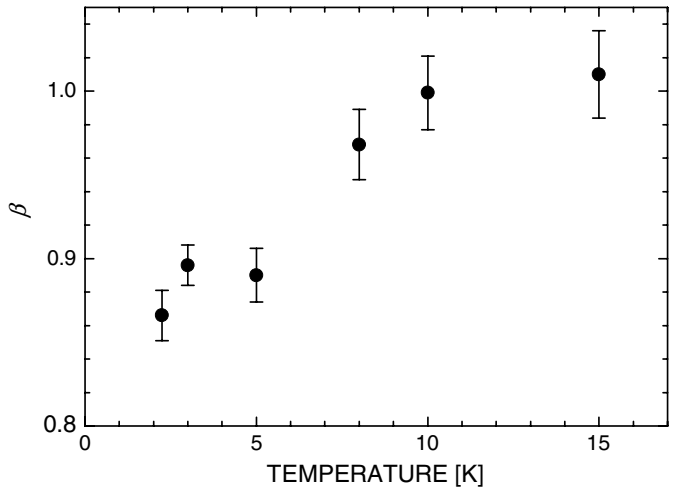

Figure 6. The temperature dependence of the stretched exponential-law coefficient β for $Yb(Cu_{0.25}Ni_{0.75})_2Si_2$.

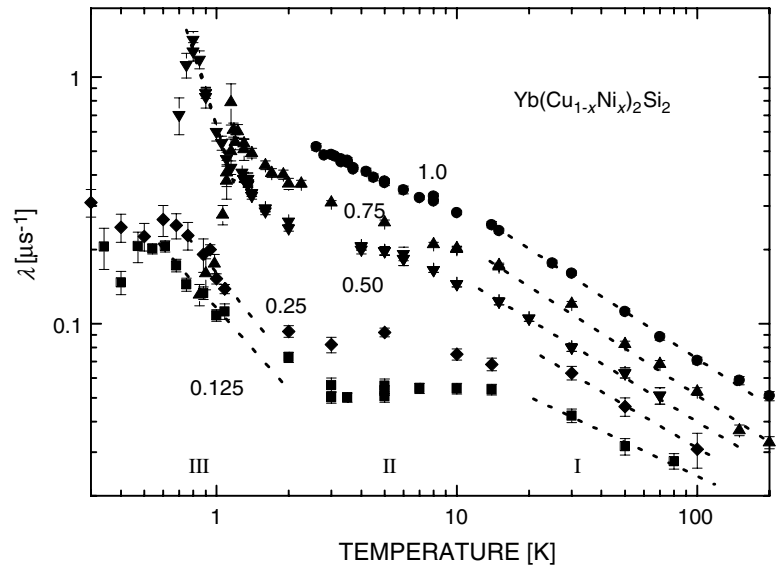

Figure 7. The temperature dependence of the ZF relaxation rate λ for selected $Yb(Cu_{1-x}Ni_x)_2Si_2$ samples. The lines are guides to the eye.

3.3. Yb dynamics in the paramagnetic regime

The dynamics of the Yb magnetic moments was investigated in LF by performing temperature scans with $B_{ext} = 2$ kG and by determining the field dependence (up to $B_{ext} = 6$ kG) at 5 K. The LF μSR spectra are best fitted using an exponential depolarization function:

$$P(t) = \exp(-\lambda_{LF}t). \tag{2}$$

This equation corresponds to the case $\beta = 1$, which has been seen to be valid from a few degrees above T_m. As the external applied field quenches any static contribution, the observed

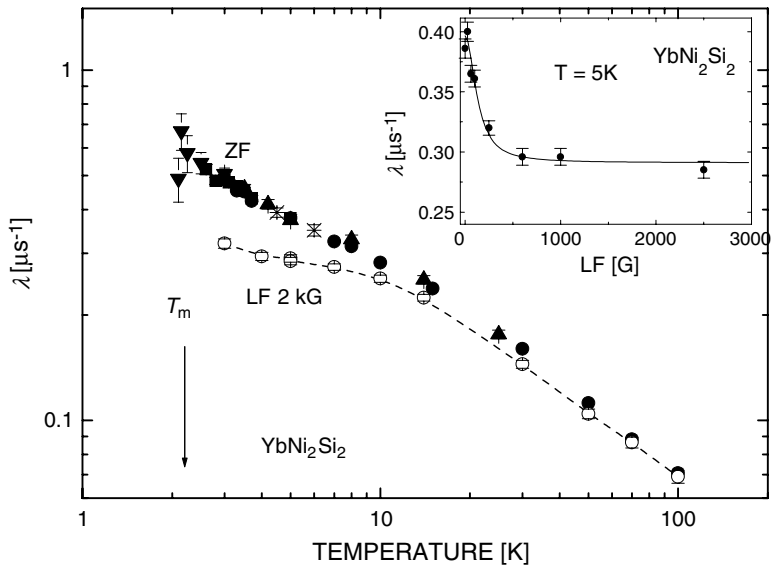

Figure 8. The temperature dependence of the ZF (closed symbols, different symbols indicating results obtained on different μSR spectrometers) and LF (open symbols) μ^+ relaxation rate in $YbNi_2Si_2$. The inset represents the results of the longitudinal field scan at 5 K. The curves are guides to the eye.

depolarization is due to fluctuating moments. The exponential character of the depolarization function is indicative of a sharp distribution of the depolarization rates around λ_{LF}.

The temperature dependence of the LF depolarization rates in $YbNi_2Si_2$ is reported in figure 8 together with the results of the ZF μSR measurements. A double logarithmic scale is used to enhance the details of $\lambda_{LF}(T)$ at low temperatures. The inset in figure 8 shows the field dependence of the LF depolarization rate at 5 K, indicating a fast decrease upon increasing the applied field up to 1 kG followed by saturation at higher fields.

For the samples with other concentrations, the temperature dependence of the depolarization rates is reported in figure 9, and its overall behaviour is found to be similar to the one presented above for $YbNi_2Si_2$.

3.3.1. High longitudinal fields. The absence of a sizeable field dependence of the LF depolarization rate $\lambda_{LF}(B)$ for fields larger than 1 kG is characteristic of fast and uncorrelated fluctuations of the magnetic moments surrounding the muon. One can write [24]

$$\lambda_u = \frac{M_2^{ZF}\tau_0}{1+\omega^2\tau_0^2}, \tag{3}$$

where M_2^{ZF} and τ_0 are the second moment of the 'snapshot' field distribution created by the fluctuating magnetic moments and their correlation time, respectively. $\omega/2\pi$ is the Larmor precession frequency. In the limit of fast uncorrelated spin fluctuations ($\omega^2\tau_0^2 \ll 1, \omega = \gamma_\mu B$) equation (3) becomes field independent: $\lambda_u \cong M_2^{ZF}\tau_{4f} = M_2^{ZF}/\nu_{4f}$, τ_{4f} and ν_{4f} are the correlation time and the fluctuation rate of the magnetic moments, respectively. Assuming a constant value of the fluctuating Yb moments, $1/\lambda_{LF=2\ kG}(T)$ reflects the temperature dependence of the fluctuation rate ν_{4f}. At low temperatures the $1/\lambda_{LF=2\ kG}(T)$-dependence, figure 10, is linear while at high temperatures it follows a power law with an exponent close to 0.5 ($\lambda_{LF}(T) \propto T^{-0.56}$, see the inset in figure 10).

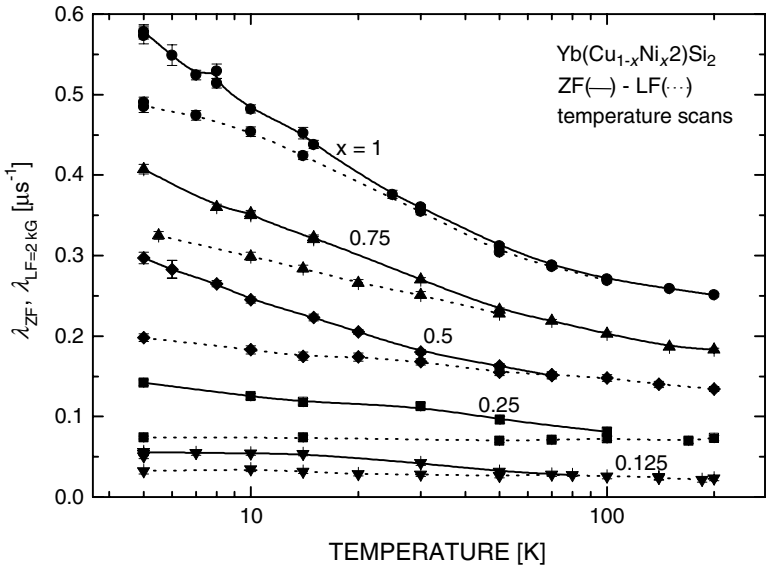

Figure 9. The temperature dependence of the μ^+ relaxation rate in ZF and longitudinal field of 2 kG. The data are translated vertically by multiple integers of 0.05 MHz (except the $x = 0.125$ data).

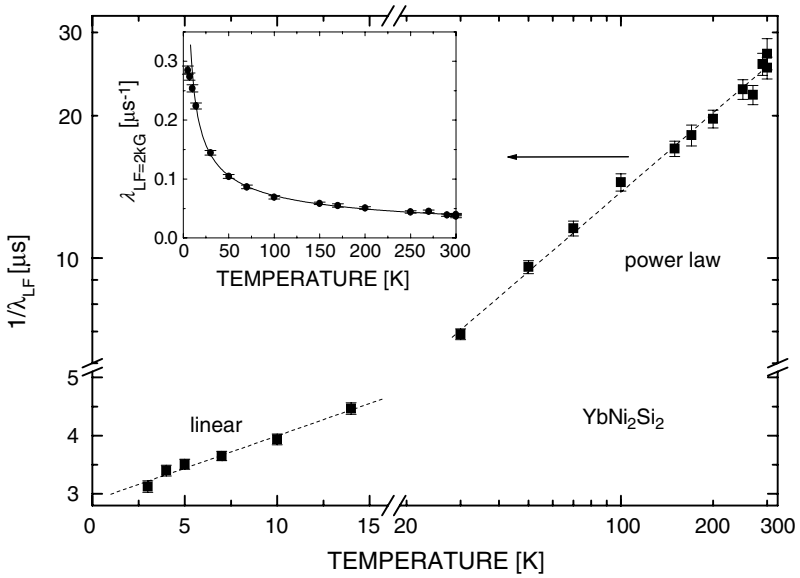

Figure 10. The $1/\lambda_{LF}(T)$-dependence (LF = 2 kG) for $YbNi_2Si_2$. The inset displays a fit of a power law with exponent -0.56 to the data.

The high temperature $\sqrt{T}$-like dependence of ν_{4f} in $YbNi_2Si_2$ is similar to that previously observed by μSR in several Kondo lattices like UCd_{11} [25], CeNiSn [26] and $YbAuCu_4$ [27]. Similar observations were reported using NMR or inelastic neutron scattering technique [28]. In an inelastic neutron scattering experiment, the quasielastic linewidth Γ^Q is a measure of the

4f spin fluctuation rate in the case of a Lorentzian shaped 4f excitation spectrum. In Kondo lattices, Γ^{Q} exhibits a $\sqrt{T}$-dependence at high temperatures [29]. The 4f spin fluctuation rate Γ^{NMR} ($\Gamma^{NMR} \propto \nu_{4f}$) of some Kondo lattice compounds, calculated from the nuclear spin–lattice relaxation measured in NMR experiments, exhibits a similar behaviour: it shows a plateau at low temperature, characteristic of a Fermi liquid behaviour, followed by a shallow minimum around the Kondo temperature T_K and a $\sqrt{T}$-behaviour at high temperatures [28]. Scaling is observed when plotting $\Gamma^{NMR}/T_0 = f(T/T_0)$ for different samples [28].

The $\sqrt{T}$ law for the fluctuation rate of the rare earth magnetic moment was predicted by Cox *et al* [30] within the framework of the degenerate Anderson one-impurity model. The model only applies to single rare earth impurities and to a degenerate ion, not taking into account the CEF splitting.

In this case, and for $T \gg T_K$, the following relation can be deduced [30]:

$$\frac{\Gamma^{NMR}(T)}{T_K} \simeq \frac{2.4}{N}\sqrt{\frac{T}{T_K}}.$$

Here N is the ground state degeneracy ($N = 8$ for a full orbital degeneracy of the ground state of Yb^{3+}).

Nevertheless, some experimental evidence indicates that single impurity calculations are relevant also to the magnetic response of Kondo lattice compounds for temperatures high above T_K.

From the $\nu_{4f}^{\mu SR}(T)/T_K = f(T/T_K)$ scaling, see figure 11, a value of $T_K = 7$ K was extracted for $YbNi_2Si_2$. Since no minimum was observed in the $\nu_{4f}(T)$-dependence for $YbNi_2Si_2$, the scaling presented in figure 11 is only approximate. However, the calculated value of T_K is of the same order of magnitude as the Kondo temperature measured for other Yb Kondo lattice systems showing magnetic ordering at low temperature (see table 1). Taking into account $T_K = 200$ K for $YbCu_2Si_2$ [40], our result points to the decrease of the Kondo temperature with increasing Ni concentration in $Yb(Cu_{1-x}Ni_x)_2Si_2$. The deviation from the pure $\sqrt{T}$ law and the absence of the minimum in the $\nu_{4f}(T)$-dependence for $YbNi_2Si_2$ might be related to the absence of full orbital degeneracy at low temperatures. It was shown (see [29] and references therein) that no minimum is expected in the $\nu_{4f}(T)$ curve for $N = 2$ ($N = 2$ at low T for $YbNi_2Si_2$). Bonville *et al* [27] invoked CEF effects to justify the absence of the minimum in $\Gamma^{Q}(T)$ and $\Gamma^{\mu SR}(T)$-dependence for $YbCu_4Al$.

A linear $\nu_{4f}(T)$-dependence such as that observed at low temperatures for $Yb(Cu_{1-x}Ni_x)_2Si_2$, see figures 10 and 12, is usually measured for relaxation rates governed by the Korringa relaxation mechanism. The Korringa fluctuation rate $\nu_{Korr} = C_K T$ represents the relaxation rate of the Yb magnetic moments due to the interaction of these magnetic moments with the conduction electrons. C_K is the Korringa constant, proportional to the second power of the product $J_{kf}N(E_F)$; see [41] and references therein. The temperature independent contribution to ν_{4f} observed in the present data points also to the presence of a RKKY relaxation mechanism due to the inter-ionic exchange.

From a $\nu_{4f} = \nu_{RKKY} + C_K T$ fit to the experimental data, figure 12, the coefficients ν_{RKKY} and C_K were obtained. They are displayed in figures 13 and 14. Both ν_{RKKY} and C_K decrease with increasing Ni concentration. As mentioned above, the Korringa constant C_K provides a direct measure of $J_{kf}N(E_F)$. A decrease of $J_{kf}N(E_F)$ with increasing Ni concentration (i.e., with the increase of the lattice pressure on the Yb ions) in the $Yb(Cu_{1-x}Ni_x)_2Si_2$ compounds is suggested by the Doniach phase diagram. It indicates the approach towards a magnetic ground state of $Yb(Cu_{1-x}Ni_x)_2Si_2$ with increasing x. This result was confirmed by μSR measurements at low temperatures, see below. In Ce compounds, the decrease of $J_{kf}N(E_F)$ when approaching the magnetic phase was demonstrated by Amato [42] for $CeCu_{5-x}Al_x$. In

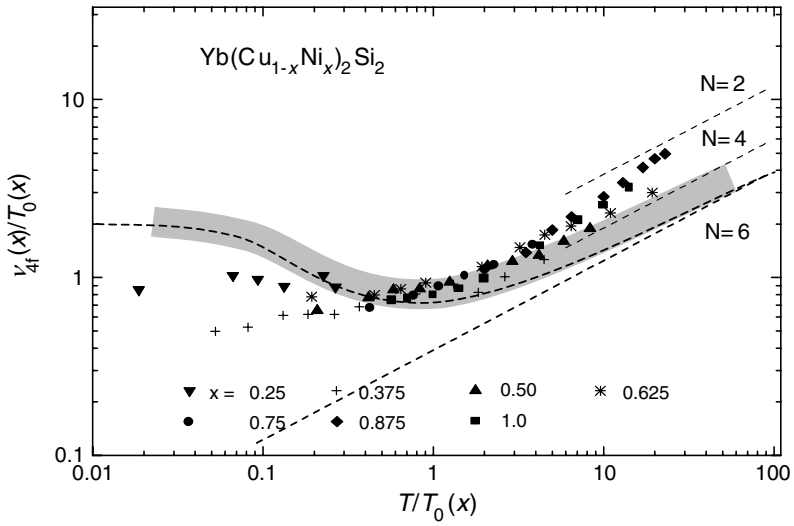

Figure 11. The $\nu_{\mathrm{f}}^{\mu\mathrm{SR}}(T)/T_{\mathrm{K}} = f(T/T_{\mathrm{K}})$ scaling for $Yb(Cu_{1-x}Ni_x)_2Si_2$, show by different symbols for different values of x. The scaling $\Gamma^{\mathrm{NMR}}(T)/T_0 = f(T/T_0)$ for different Ce and Yb compounds (shaded curve, from [28]) is also presented.

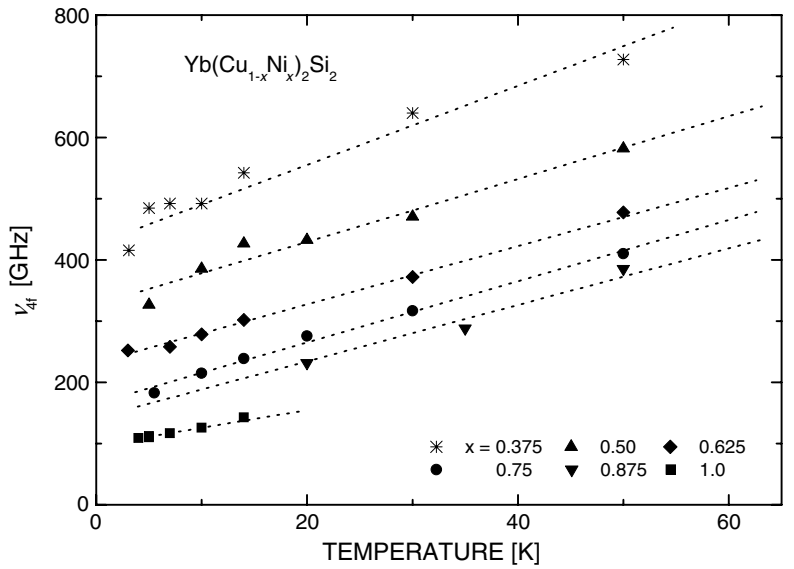

Figure 12. The $\nu_{4\mathrm{f}}(T)$-dependence for different Ni concentrations. The lines represent fits to the data (see text).

that case, the $[J_{kf}N(E_{\mathrm{F}})](x)$-dependence was obtained from the hyperfine coupling constant A_{c} calculated from the temperature dependence of the muon Knight shift.

3.3.2. Low longitudinal fields. We turn now to the discussion of the field scans performed at 5 K, more precisely to the $\lambda_{\mathrm{LF}}(B)$-dependencies up to 1 kG. As mentioned above, for all the samples with $x > 0$, $\lambda_{\mathrm{LF}}(B)$ measured at 5 K shows a fast decrease with the increase of

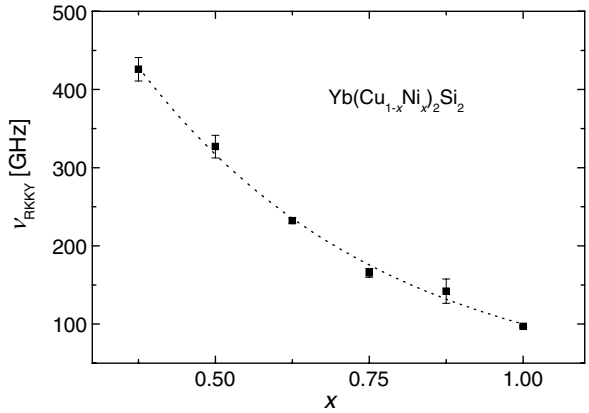

Figure 13. $\nu_{\mathrm{RKKY}}(x)$ for $Yb(Cu_{1-x}Ni_x)_2Si_2$. The curve is a guide to the eye.

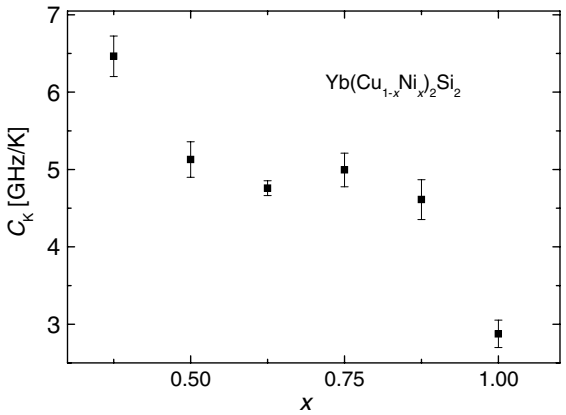

Figure 14. The dependence of the Korringa constant C_{K} on the Ni concentration in $Yb(Cu_{1-x}Ni_x)_2Si_2$.

Table 1. Characteristic temperatures for different Yb compounds showing magnetic ordering at low temperatures.

	T_{K} (K)	T_{m} (K)	References
YbSi	2.5	1.6	[31]
YbBiPt	1–10	0.4	[32]
YbBiPd	8	<2	[33, 34]
YbNiAl	3	3	[35, 36]
YbPdSb	7	1	[36]
YbP	10	0.7	[37, 38]
YbN	5	0.9	[37]
YbNiSn	0.7	5.7	[39]
$YbCu_4Au$	20	0.5	[27]
$YbNi_2Si_2$	>7	2.1	[5], this work

the applied field followed by saturation at fields higher than 1 kG. One should keep in mind that a longitudinal field as low as 10 G decouples from the μ^+ depolarization rate the static

field contribution stemming from the nuclear magnetic moments. Hence the reported field dependence cannot be connected to such a decoupling.

Because of its strong field dependence, we consider that the observed $\lambda_{LF}(B < 1\ kG)$ is due to a slow fluctuating component of the magnetic field at the muon site. This component may originate either from fluctuations of the nuclear moments induced by the fluctuating Yb^{3+} magnetic moments, from correlated fluctuations of the Yb^{3+} moments, or from another mechanism. The hypothesis of induced nuclear moment fluctuations can be safely excluded since the value of the second moment of the field distribution created by the nuclear moments, $M_2^{ZF} = 1.24\ MHz^2$, computed from a fit of equation (3) to $[\lambda_{LF}(B) - \lambda_{LF}(2\ kG)]$ is about one order of magnitude larger that the calculated value for the 4e or the 8g sites.

By taking into account the possibility of correlated fluctuations, the situation can be viewed as follows: at high temperatures, the spins fluctuate in a completely uncorrelated manner and cause statistically independent contributions to the components of the fluctuating hyperfine fields at the muon site. With decreasing temperature, the paramagnetic spins develop parallel (antiparallel) correlations like in ferromagnets (antiferromagnets) resulting in field components B_c oscillating with a frequency ν_c distinct from the fast oscillating uncorrelated moments. We have used a modified equation (3) [43] to describe the relaxation rate due to the correlated fluctuations:

$$[\lambda_{LF}(B) - \lambda_{LF}(2\ kG)] = \lambda_c = \frac{2}{3}\frac{\gamma_\mu^2 B_c^2 \tau_c}{1 + \omega^2 \tau_c^2}, \tag{4}$$

and therefore

$$\lambda_{LF}(B) = M_2^{ZF}\tau_0 + \frac{2}{3}\frac{\gamma_\mu^2 B_c^2 \tau_c}{1 + \omega^2 \tau_c^2}, \tag{5}$$

where B_c describes the amplitude of the correlated part of the local fluctuating magnetic field and τ_c its correlation time. If B_c is small we can assume that $M_2^{ZF}(T)$ stays constant over the investigated temperature range (see the discussion about equation (3)). In $YbNi_2Si_2$, the Yb^{3+} magnetic moments order helically below T_m [6]. The magnetic structure can be described as ferromagnetic a–b planes rotated along the c-direction. Increasing spin–spin correlations increase the value of B_c since the muon site is close to the a–b plane and contains a second order symmetry axis for the Yb structure, i.e., the magnetic fields produced by the in-plane ferromagnetic arrangement of the Yb^{3+} magnetic moments add constructively. From the fit of equation (4) to the $\lambda_c(B)$ data for $YbNi_2Si_2$, figure 15, values of 16 G for B_c and 12 MHz for ν_c $(=1/\tau_c)$ were obtained. $B_c(x)$ and $\nu_c(x)$ are displayed in figures 16 and 17, respectively. Theoretically, the value of B_c increases from zero, i.e., uncorrelated fluctuations for $YbCu_2Si_2$, to several kG, the value of the local field in the magnetic phase for fully correlated fluctuations in $YbNi_2Si_2$ below 2 K. With $B_c = 16$ G at 5 K for $YbNi_2Si_2$ the magnetic correlations between the Yb^{3+} moments are still weak. While the increase of B_c with increasing Ni concentration reflects the increase of the correlations strength between the Yb ions, the similar increase of $\nu_c(x)$ is not fully understood. The reader should keep in mind that ν_0 $(=1/\tau_0)$, the fluctuation rate of the electronic magnetic moments, decreases with increasing Ni concentration in $Yb(Cu_{1-x}Ni_x)_2Si_2$.

3.4. ZF μSR in the magnetic phase ($T < T_m$)

The μSR measurements at low temperatures indicate that magnetic ordering occurs in all samples with $x \geqslant 0.125$. The signature of the magnetic order in the μSR spectra is a fast relaxing Gaussian-like component, see figure 18, suggesting that the field distribution at the muon site is broad. The broad field distribution at the muon site and the absence of the wiggles

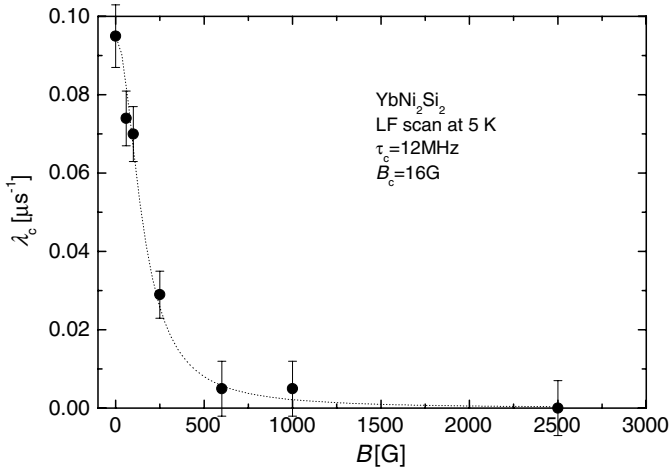

Figure 15. The $\lambda_c(B)$-dependence for $YbNi_2Si_2$. The dotted curve is a fit of equation (4) to the experimental data.

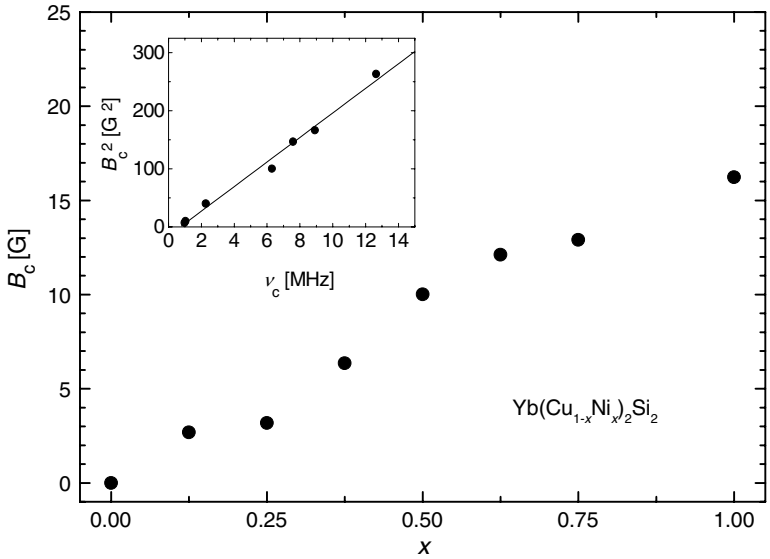

Figure 16. The $B_c(x)$-dependence for $Yb(Cu_{1-x}Ni_x)_2Si_2$. The inset shows the $B_c^2(\nu_c)$-dependence with x as implicit parameter.

in the μSR spectra originates from both the magnetic structure (helical for $YbNi_2Si_2$ [6]) and the lattice defects introduced by the chemical substitution. Below the magnetic transition temperature T_m, the μSR spectra were best fitted using

$$A P_z(t) = A_{para}\left(\tfrac{1}{3} + \tfrac{2}{3}(1-\Delta^2 t^2)e^{-\Delta^2 t^2/2}\right)e^{-(\lambda t)^\beta} + A_{mag}\left(\tfrac{1}{3}e^{-\lambda_m t} + \tfrac{2}{3}e^{-\sigma_m^2 t^2/2}\right), \quad (6)$$

where $A_{para} + A_{mag} = A$ is the full asymmetry (obtained from fits to the μSR spectra for $T > T_m$). The first term on the right-hand side of equation (6), describing the paramagnetic fraction of the sample, is identical to that given by equation (1), while the second term accounts for the magnetic phase. λ_m represents the μ^+ depolarization rate stemming from dynamical

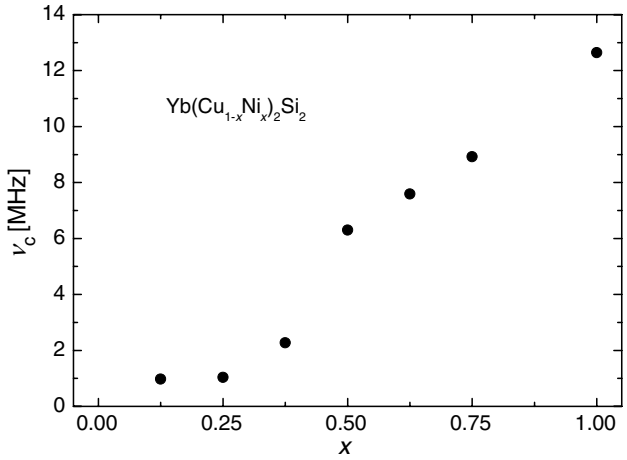

Figure 17. The $\nu_c(x)$-dependence for Yb(Cu$_{1-x}$Ni$_x$)$_2$Si$_2$.

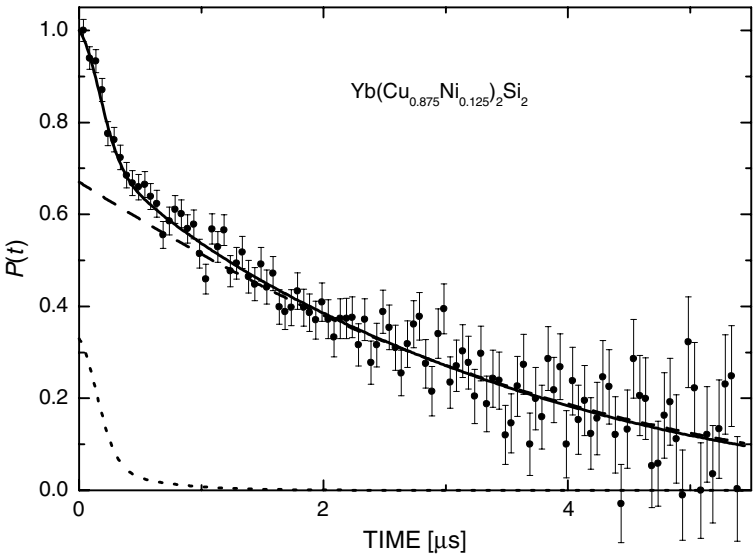

Figure 18. Typical μSR spectra for $T < T_m$ in Yb(Cu$_{1-x}$Ni$_x$)$_2$Si$_2$. The different components of the fit function are described in the text.

processes while σ_m is the depolarization rate due essentially to the field distribution created by the electronic moments. The ratio A_{mag}/A defines the fraction of the sample that is subject to magnetic ordering.

The temperature dependence of A_{mag}/A for different Ni concentrations is presented in figure 19. The curves are fits with a phenomenological function of the form

$$\frac{A_m}{A}(T,x) = \frac{a(x)}{1+e^{b(x)(T-T_m(x))}}, \tag{7}$$

where $a(x)$ represents the magnetic fraction of the sample, $T_m(x)$ the transition temperature and b is a fit parameter that describes the width of the transition. The $T_m(x)$-dependence is plotted in figure 20. The increase of T_m with x indicates the gradual change of the balance between

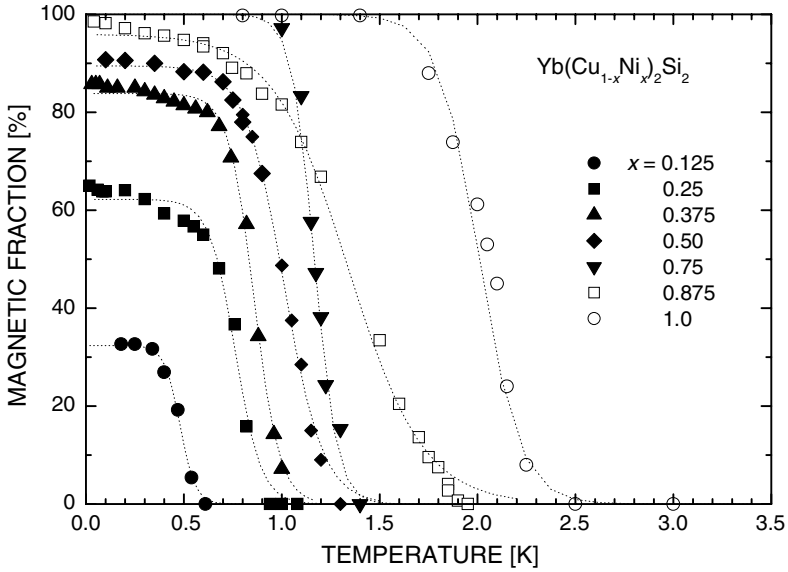

Figure 19. The temperature dependence of the magnetic fraction of the sample, A_{mag}/A.

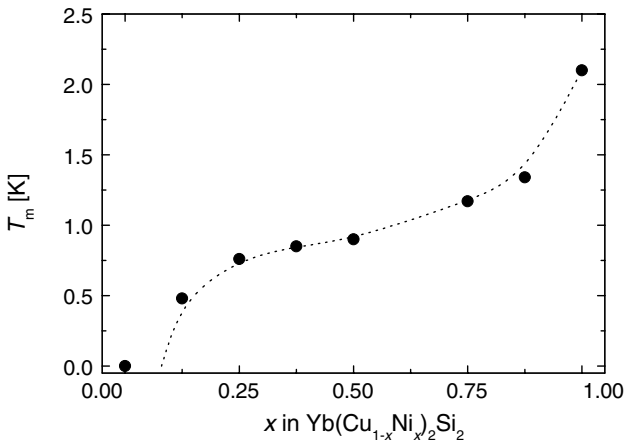

Figure 20. The Ni concentration (x) dependence of the magnetic transition temperature in $Yb(Cu_{1-x}Ni_x)_2Si_2$. The curve is a guide to the eye.

the Kondo and the RKKY interaction in $Yb(Cu_{1-x}Ni_x)_2Si_2$. The zero value of $T_m(x = 0.08)$ is based on μSR measurements of a sample with $x = 0.08$, which do not show any sign of magnetic ordering down to 40 mK.

It is evident from figure 19 that magnetic correlations develop in a fraction of the sample volume which increases with increasing Ni concentration. For $x = 0.5$ almost the entire sample is magnetic below T_m. It was found [9] that A_{mag}/A scales well with the probability for a Yb ion to have at least two Ni ions as nearest neighbours. The probability $P_N(n, x)$ for the Yb ion to have a number n of Ni neighbours in a $Yb(Cu_{1-x}Ni_x)_2Si_2$ compound is given by

$$P_N(n, x) = \frac{N!}{n!(N-n)!}x^n(1-x)^{N-n},$$

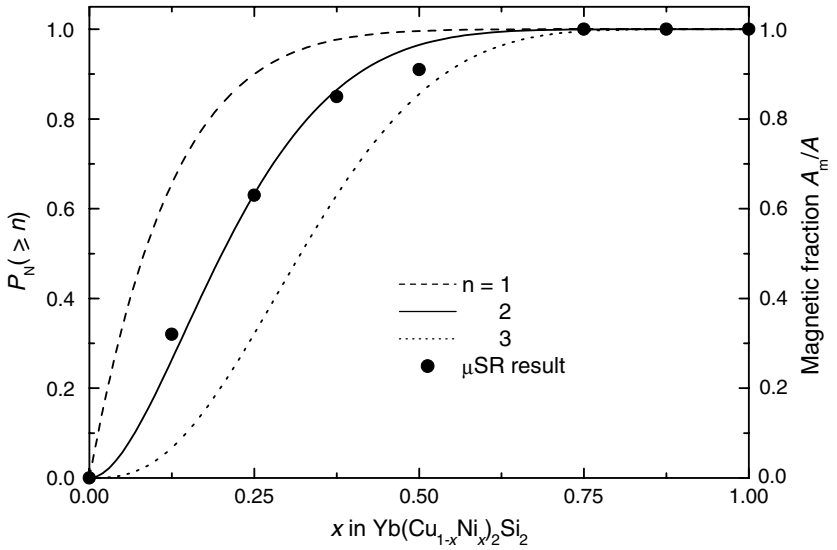

Figure 21. The calculated probability for an Yb ion to have at least n Ni ions as nearest neighbours, as a function of the Ni concentration in $Yb(Cu_{1-x}Ni_x)_2Si_2$ (curves). The empiric fraction of the sample that presents magnetic ordering at low temperatures, A_{mag}/A is represented by bullets.

and the probability to have at least n Ni neighbours can be easily calculated by summation:

$$P_N(\geqslant n, x) = \sum_{i=n}^{N} \frac{N!}{i!(N-i)!} x^i (1-x)^{N-i}.$$

The probability of an Yb ion to have $n = 1, 2$ and 3 Ni nearest neighbours at different Ni concentrations is displayed in figure 21 together with the experimental value of $A_{mag}/A(x)$.

A similar scaling procedure was used by Jaccarino and Walker [44] to describe the discontinuous occurrence of localized moments in certain alloys. It was assumed that the distinction between different impurity ions is based on the nature of their local environment in the disordered alloy and was considered that in some environments the ions are unmagnetized and in all others they have their full magnetic moment. The model to describe the different environments is similar to that presented above. However, an important distinction needs to be made between the two approaches, although the mathematical procedure is similar: in the Jaccarino–Walker model the *occurrence of the magnetic moment* on the respective ion is determined by its environment, while in $Yb(Cu_{1-x}Ni_x)_2Si_2$ the Yb ion has a magnetic moment and the environment sets the necessary condition for having a *magnetic ordering of the moment*.

The depolarization rate σ_m due to the electronic moments increases exponentially with increasing Ni concentration as shown in figure 22. As stated above, the depolarization rate σ_m in the magnetic phase reflects the second moment of the field distribution arising from the Yb 4f moments. The fast increase of σ_m with x can be related to the increase of the ordered moment due to the change in the balance of the Kondo and the RKKY interactions. At low Ni concentrations a cluster type of magnetic ordering might occur, with reduced magnetic moments due to the Kondo effect. The size of the clusters should not play a significant role in the $\sigma_m(x)$-dependence since no change of slope was observed around $x = 0.5$, the Ni concentration at which the magnetism occurs in the entire volume of the sample. On the other hand, two distinct regimes are observed in the $T_m(\sigma_m)$-dependence presented in figure 23. A fast increase of the transition temperature T_m in the range of small Yb moments is followed

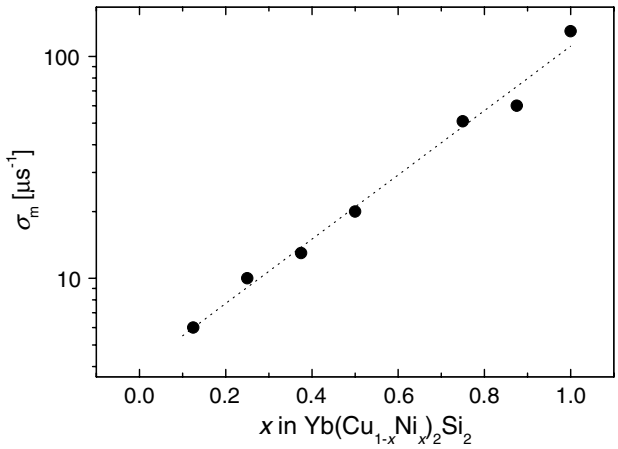

Figure 22. The $\sigma_m(x, T \to 0)$-dependence in $Yb(Cu_{1-x}Ni_x)_2Si_2$.

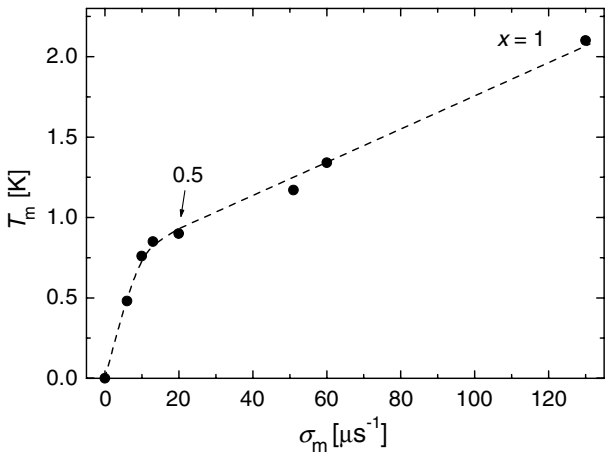

Figure 23. The magnetic transition temperature T_m as a function of the low-T μ^+ depolarization rate, $\sigma_m(x, T \to 0)$ for $Yb(Cu_{1-x}Ni_x)_2Si_2$. The curves are guides for the eye.

by a slope change above $x = 0.375$. For both regions, a linear $T_m(\sigma_m)$-dependence appears to be a good approximation.

3.5. Chemical substitution versus external pressure

By comparing the pressure dependence of the unit-cell volume of $YbCu_2Si_2$ [45] with the cell volume of the corresponding compound with partial chemical substitution of Cu by Ni, figure 24, we obtain the $p_x(p_{ext})$ correspondence curve, see figure 25. p_x is the 'lattice pressure' caused by the chemical substitution while p_{ext} is the external pressure leading to the same cell volume for pressurized but non-substituted $YbCu_2Si_2$. Note the slope change in the $p_x(p_{ext})$-dependence at $p_{ext} = 80$ kbar, the pressure above which pressure-induced magnetic ordering was observed in $YbCu_2Si_2$ [45]. The corresponding $p_x = 0.5$ represents the value of the Ni concentration for which almost the entire sample has a magnetic ground state.

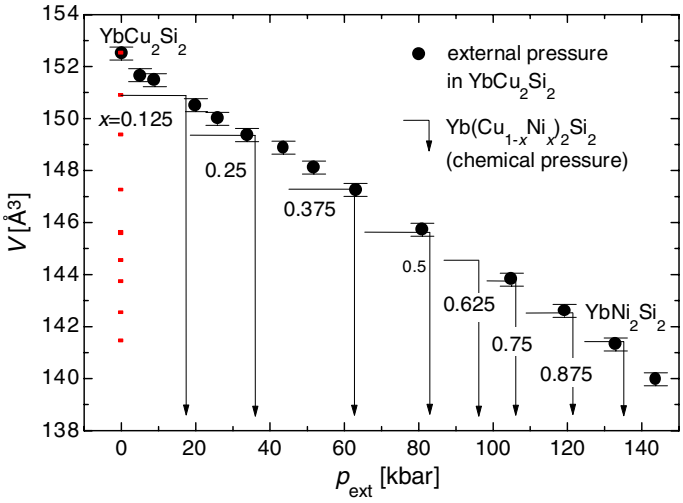

Figure 24. The pressure variation of the unit-cell volume of $YbCu_2Si_2$ (black points, data taken from [45]). The correspondence between the external pressure p_{ext} and the chemical pressure p_x (Ni concentration) which produces the same volume change is marked with arrows.

(This figure is in colour only in the electronic version)

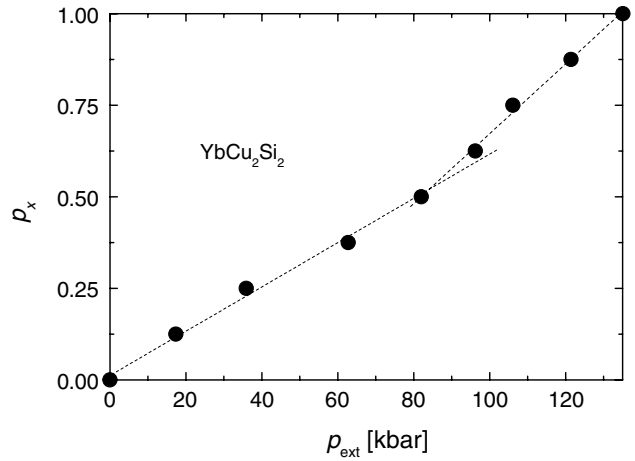

Figure 25. The correspondence between the chemical pressure p_x (Ni concentration) and the external pressure p_{ext} that produces the same volume effect.

The unit cell volume of $YbNi_2Si_2$ ($x = 1$, $T_m = 2.1$ K) corresponds to that of $YbCu_2Si_2$ under a pressure of 135 kbar ($T_m \cong 5$ K, [45]). The reduction of the transition temperature of $YbNi_2Si_2$ compared to that of $YbCu_2Si_2$ compressed to the same volume can be related to the electron doping caused by the substitution of Cu by Ni. Similar effects observed in $YbCu_{5-x}Al_x$ [46] indicate that electron doping introduced by the chemical substitution compete with volume effects for establishing the ground state of the system.

4. Conclusions

The main result of this investigation is that magnetic ordering occurs in an unusual way upon the substitution of Cu by Ni in the nonmagnetic compound $YbCu_2Si_2$. In $Yb(Cu_{1-x}Ni_x)_2Si_2$ ($x > 0$) only a fraction of the sample orders magnetically at low temperature. The magnetic fraction of the sample scales with the probability for an Yb ion to have at least two Ni ions as nearest neighbours. There is no correspondent of this phase separation in the paramagnetic phase, i.e., the distribution of the fluctuation rate of the Yb^{3+} magnetic moments is quite sharp, suggesting that the magnetic clustering takes place in a small temperature interval around T_m. However, correlated fluctuations—but with small values of the resulting correlated fields and fluctuation rates—were observed at low temperatures.

The Cu substitution by Ni in $YbCu_2Si_2$ favours a magnetic ground state. This effect was expected according to the Doniach phase diagram since lattice pressure is created on the Yb ions in $Yb(Cu_{1-x}Ni_x)_2Si_2$ while increasing the Ni concentration. The lattice pressure modifies the balance between the Kondo and the RKKY interactions in the favour of the latter one. The decrease of the Kondo temperature, obtained from a $\nu_{4f}^{\mu SR}(T)/T_K = f(T/T_K)$ scaling, with increasing Ni concentration supports the above assumptions.

Acknowledgments

We thank J Sierro and D Jaccard for valuable discussions and help during the sample preparation and characterization. The work was performed at the Swiss Muon Source, Paul Scherrer Institute, Villigen, Switzerland and partially at ISIS-RAL UK. Two of us (DA and AA) are grateful to the ESF (project FERLIN) for financial support.

References

[1] Doniach S 1977 *Physica* B **91** 231
[2] Alami-Yadri K and Jaccard D 1996 *Solid State Commun.* **100** 385
[3] Sales B C and Wiswanathan R 1976 *J. Low Temp. Phys.* **23** 449
[4] Neumann G, Langen J, Zahel H, Plumacher D, Kletowski Z, Schlabitz W and Wohlleben D 1985 *Z. Phys.* B **59** 133
[5] Bonville P, Hodges J A, Imbert P, Jehanno G, Jaccard D and Sierro J 1991 *J. Magn. Magn. Mater.* **97** 178
[6] André G, Bonville P, Bourée F, Bombik A, Kolenda M, Oleś A, Pacyna A, Sikora E and Sztyula A 1995 *J. Alloys Compounds* **224** 253
[7] Jaccard D 1981 *PhD Thesis* University of Geneva
[8] Alami-Yadri K, Jaccard D and Andreica D 1999 *J. Low Temp. Phys.* **114** 135
[9] Andreica D, Alami-Yadri K, Jaccard D, Amato A and Schenck A 1999 *Physica* B **259–261** 144
[10] Andreica D 2001 *PhD Thesis* IPP/ETH-Zurich
[11] Andreica D, Amato A, Gygax F, Pinkpank M and Schenck A 2000 *Physica* B **289/290** 24
[12] Kubo R and Toyabe T 1967 *Magnetic Resonance and Relaxation* ed R Bline (Amsterdam: North-Holland)
[13] Schenck A 1985 *Muon Spin Spectroscopy: Principles and Applications in Solid State Physics* (Bristol: Hilger)
[14] Abela R, Amato A, Baines C, Donath X, Erne R, George D C, Herlach D, Irminger G, Reid I D, Renker D, Solt G, Suhi D, Werner M and Zimmermann U 1999 *Hyperfine Interact.* **120/121** 575
[15] Feyerherm R 1995 *PhD Thesis* IPP/ETH-Zurich
[16] Amato A *et al* 1993 *PSI Newslett.* 1 89
[17] Amato A, Feyerherm R, Gygax F N and Schenck A 1997 *Hyperfine Interact.* **104** 115
[18] Yamamoto Y, Marumoto K, Miyako Y, Nishiyama K and Nagamine K 1997 *Hyperfine Interact.* **104** 227
[19] MacLaughlin D E, Cooke D W, Heffner R H, Hutson R L, McElfresh M W, Schillaci M E, Rempp H D, Smith J L, Willis J O, Zirngiebl E, Boekema C, Lichti R L and Oostens J 1988 *Phys. Rev.* B **37** 3153
[20] Pomjakushin V Yu, Balagurov A M, Raspopina E V, Sikolenko V V, Gribanov A V, Schenck A, Amato A, Zimmermann U and Lyubutin I S 2000 *J. Phys.: Condens. Matter* **12** 7969

[21] Campbell I A, Amato A, Gygax F N, Herlach D, Schenck A, Cywinski R and Kilcoyne S H 1994 *Phys. Rev. Lett.* **72** 1291
[22] Pinkpank M 2000 *PhD Thesis* IPP/ETH-Zurich
[23] Goremychkin E A and Osborn R 2000 *J. Appl. Phys.* **87** 6818
[24] Slichter C 1990 *Principles of Magnetic Resonance* (Berlin: Springer)
[25] Barth S, Ott H R, Gygax F N, Schenck A, Rice T M and Fisk Z 1986 *Hyperfine Interact.* **31** 397
[26] Kalvius G M, Kratzer A, Wäppling R, Takabatake T, Nakamoto G, Fujii H, Kiefl R F and Kreitzmann S R 1995 *Physica* B **206/207** 807
[27] Bonville P, Dalmas de Réotier P, Yaouanc A, Polatsek G, Gubbens P C M and Mulders A M 1996 *J. Phys.: Condens. Matter* **8** 7755
[28] Qachaou A, Beaurepaire E, Benakki M, Lemius B, Kappler J P, Meyer A J P and Panissod P 1987 *J. Magn. Magn. Mater.* **63/64** 635
[29] Panissod P, Benakki M and Qachaou A 1988 *J. Physique Coll.* **49** C8 685
[30] Cox D L, Bickers N E and Wilkins J W 1985 *J. Appl. Phys.* **57** 3166
[31] Bonville P, Gonzalez-Jimenez F, Imbert P, Jaccard D, Jehanno G and Sierro J 1989 *J. Phys.: Condens. Matter* **1** 8567
[32] Canfield P C, Movshovich R, Robinson R A, Thompson J D, Fisk Z, Beyermann W P, Lacerda A, Hundley M F, Heffner R H, MacLaughlin D E, Trouw F and Ott H R 1994 *Physica* B **197** 101
[33] Aliev F G *et al* 1989 *Sov. Phys.—Solid State* **31** 1615
[34] Dhar S K, Nambudripad N and Vijayaraghavan R 1988 *J. Phys. F: Met. Phys.* **18** L41
[35] Schank C, Olesch G, Kohler J, Tegel U, Klinger U, Diehl J, Klimm S, Sparn G, Horn S, Geibel C and Steglich F C 1995 *J. Magn. Magn. Mater.* **140–144** 1237
[36] le Bras G, Bonville P, Besnus M J, Haen P, Imbert P, Polatsek G and Aliev F G 1995 *Physica* B **206/207** 338
[37] le Bras G, Bonville P, Hodges J A, Imbert P, Polatsek G, Fischer P, Keller L, Donni A, Kohgi M and Suzuki T 1993 *Physica* B **190** 333
[38] Donni A, Fischer P, Furrer A, Bonville P, Hulliger F and Ott H R 1990 *Z. Phys.* B **81** 83
[39] Bonville P, Polatsek G, Hodges J A, Imbert P and le Bras G 1993 *Physica* B **186–188** 254
[40] Tomala K, Weschenfelder D, Czjzek G and Holland-Moritz E 1990 *J. Magn. Magn. Mater.* **89** 143
[41] Schenck A and Gygax F N 1995 Magnetic materials studied by muon spin rotation spectroscopy *Handbook of Magnetic Materials* vol 9, ed K H J Buschow (Amsterdam: Elsevier) pp 57–302
[42] Amato A 1998 private communication
[43] Pinkpank M, Amato A, Gygax F N, Schenck A, Henggeler W and Fischer P 1997 *Hyperfine Interact.* **105** 145
[44] Jaccarino V and Walker L R 1965 *Phys. Rev. Lett.* **15** 258
[45] Winkelmann H, Abd-Elmeguid M M, Micklitz H, Sanchez J P, Vulliet P, Alami-Yadri K and Jaccard D 1999 *Phys. Rev.* B **60** 3324
[46] Bauer E, Hauser R, Galatanu A, Michor H, Hilscher G, Sereni J, Berisso M G, Pedrazzini P, Galli M, Marabelli F and Bonville P 1999 *Phys. Rev.* B **60** 1238